Effect of the geomagnetic field on
the intensity of sodium laser guide stars

N.Moussaoui[1], R. Holzlöhner[2], W.Hackenberg[2], D. Bonaccini Calia[2]

[1] Faculty of Physics, University of Sciences and Technology Houari Boumediene
BP32 El-Alia, Bab-Ezzouar, Algiers, Algeria
[2] European Southern Observatory, Karl-Schwarzschild-Straße 2, D-85748
Garching bei München, Germany

ABSTRACT

In calculating the return flux of sodium laser guide stars (LGS), often only the best return conditions are assumed, relying on strong optical pumping with a circularly polarized laser. However, one can obtain this optimal return only along one specific laser orientation on the sky, depending on the direction of the geomagnetic field. Sodium atoms precess around magnetic field lines which cycles the magnetic quantum number, reducing the effectiveness of optical pumping. The risk is hence for the system designer to overestimate the effective return flux for a given laser power.

In this paper we present calculations for the effect of the geomagnetic field on the return flux. Optical pumping actually produces little improvement in most observing directions. In addition, we find that at many observatory locations, the direction of optimal return flux is very close to the horizon, often below the observing limit.

Key words: sodium laser guide stars, optical pumping, sodium atoms, geomagnetic field, adaptive optics.

1. INTRODUCTION

The CW sodium LGS return flux depends on a various number of parameters: the launched laser beam power, laser spectrum and polarization, LGS spot size at the layer, atmospheric transmission, layer distance, sodium column density and rates for atomic collisions and spin depolarization. Furthermore optical pumping, atomic recoil and saturation effects of the sodium atoms have to be taken into account.

Optical pumping of atomic sodium with circularly polarized light can increase the effective absorption cross section theoretically by a factor of more than 2 compared to non-polarized excitation of the $F = 2$ hyperfine ground state[1]. The increase on the return light for circularly over linearly polarized light has been reported by Ge et $al.$[2] to be 30%, Rabien et $al.$[3] find 30–50%. Denman et $al.$[4] measured a return flux increase of factor 2.25 at the Starfire Optical Range (SOR) when switching from linear to circular polarization. The exact gain value reached in praxis strongly depends on the CW laser spectral format and the atomic spin relaxation. The latter is mainly caused by the atomic spin precession in the earth's magnetic field. In this context it has to be pointed out that it is possible to optically pump the entire Doppler-broadened absorption profile Quivers[5]. For a laser spectral format that does not cover the entire Doppler-broadened profile, most efficient use of optical pumping is made if some laser light (~ 10%) is used for the simultaneous excitation of the $F = 1$ hyperfine ground state in order to pump back spin-depolarized atoms.

The geomagnetic field intensities and orientations are obtained from the British Geological Survey website[6]. For our calculations, firstly we set the LGS intensity due to all the other factors is 100%. The geomagnetic field reduces this intensity. Secondly we introduced the effect of the atmospheric transmission on the laser beam propagation. We calculated the combined effect of the geomagnetic field and the atmospheric transmission on the enhancement of the sodium LGS return due to optical pumping.

In Section 2, we present the characteristics of the mesospheric sodium layer. In Section 3, we present the laser excitation of the sodium atoms and especially the optical pumping effect in detail. Section 4 presents the effect of the geomagnetic field on the circularly polarized optical pumping of the mesospheric sodium atoms. Finally we present in Section 5 our results about the effect of the geomagnetic field and the airmass on the intensity of the sodium LGS for several telescopes.

2. MESOSPHERIC SODIUM LAYER

The input of meteoric material into the Earth's atmosphere is believed to be the origin of the mesospheric sodium layer, Plane[7]. This happens because below the mean altitude of the sodium layer 92 km, Davis et al.[8], the atmospheric pressure begins to become significant, which leads to frictional heating of the meteoric material. The meteoric ablation provides a continuous large flux of metallic vapor entering the Earth's atmosphere. Sodium is one of the constituents of meteorites and accounts for about 0.6% of the total material. Although the total amount of the sodium in the mesosphere is very small, only about 600 kg in the entire mesosphere, its resonant cross-section is sufficiently large that it can scatter a few percent of the energy of a laser beam tuned to its D_2 line, Kibblewhite[9].

The balance of the sodium density at the mesospheric sodium layer is controlled by the meteoric ablation input and various sink mechanisms. Previous studies show that temperature dependent chemistry plays a significant role in changing sodium density which further leads to the seasonal sodium layer abundance variations because of seasonal variation of mesospheric layer temperature Plane[7]. The sodium column density is around 5×10^{13} atoms/m^2, and the temperature is about 200 K, Gardner et al.[10], Fricke et al.[11]. The range of velocities of the sodium atoms characterized by this temperature corresponds to a range of frequency shifts for the homogeneous absorption profiles of the sodium atoms (Doppler broadening) of 1.07 GHz full width at half maximum (FWHM). The Doppler-broadened absorption profile is referred to as inhomogeneously broadened because different velocity atoms have different center absorption frequencies. The combined ground and excited–state hyperfine-level energy separations and the Doppler broadening result in an absorption profile with $\Delta\nu_D = 3$ GHz FWHM. Because the mesospheric sodium column density per natural linewidth of 10 MHz is 1.7×10^{11} atoms/m^2 and the single-atom absorption cross section is 1.7×10^{-13} m^2, only about 3% of vertically propagating resonance radiation is absorbed and reradiated by the sodium atom layer.

At altitudes between 85 and 95 km, the atmospheric gas number density varies from 1.7×10^{20} to 2.9×10^{19} m^{-3}. Therefore the mean collision time between the sodium atoms and the atmospheric gas molecules varies from 27 μs to 155 μs, Jeys[12]. Collisional rates at the sodium layer are too slow to affect the D_2 absorption or emission directly.

The general characteristics of the mesospheric sodium layer (vertical density distribution and temperature) at mid-southern latitudes are very similar to those measured at mid-northern latitudes, except for a phase shift of 6 months for the season-dependent parameters Clemesha and Takahashi[13], Qian and Gardner[14], Clemesha, Batista and Simonich[15], Butler et al.[16], O'Sullivan et al.[17].

3. OPTICAL PUMPING OF THE MESOSPHERIC SODIUM ATOMS

Atomic sodium has a total of 11 electrons with a single valence electron outside closed shells. The complete term symbol of the ground state is $1s^2\,2s^22p^63s\ ^2S_{1/2}$, and of the first excited state, $1s^2\,2s^22p^63s\ ^2P_{1/2,3/2}$. The interaction of the magnetic moment of the electron with the magnetic field associated with the orbital motion of the electron leads to the energy level splitting within the first excited state, $3^2P_{1/2}$, $3^2P_{3/2}$. The two states are separated in energy by about 520 GHz. The transitions between the upper state $3^2P_{3/2}$ and the ground state $3^2S_{1/2}$ cause the sodium D_2 emission or absorption at 0.5890 μm, while the transitions between the lower state $3^2P_{1/2}$ and the ground state causes the sodium D_1 emission or absorption at 0.5896 μm.

The total electron angular momentum of the ground state and first excited state are $J = 1/2$ and $J = 1/2,\ 3/2$, respectively. Naturally occurring sodium is composed of virtually 100% one isotope, which has a nuclear-spin-angular-momentum quantum number $I = 3/2$. The interaction of an electron with the nuclear magnetic moment leads to the hyperfine structures associated with the ground and excited states of the sodium atom. Different hyperfine structure has a slightly different energy level. The total angular momentum quantum number including nuclear spin can be written as

$$F = I + J. \tag{1}$$

The resulting total angular momentum quantum numbers are $F = 1, 2$ for the sodium ground state, $F = 1, 2$ for the $3^2P_{1/2}$ excited state and $F = 0,1,2,3$ for the $3\ ^2P_{3/2}$ excited state. (Fig.1) shows the diagram of the sodium D transitions. The energy difference between the hyperfine state $F = 2$ and $F = 1$ in the ground state is 1.772 GHz, the energy separation for the hyperfine splitting in the $J = 1/2$ state of the first excited state is 188.6 MHz, while the energy

separations of the $J = 3/2$ state are 15.8, 34.4 and 58.3 MHz for the four hyperfine states with $F = 0,1,2,3$, respectively Arimondo et al.[18].

The sodium D_2 transitions are chosen for the generation of sodium artificial stars because they have a factor of two greater total line strength than the D_1 transitions. Furthermore, the D_2 transitions have much better optical-pumping characteristics, which results in more efficient excitation of the sodium atoms in the mesospheric sodium layer.
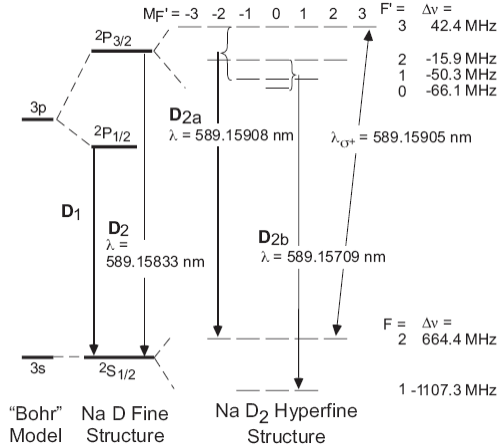

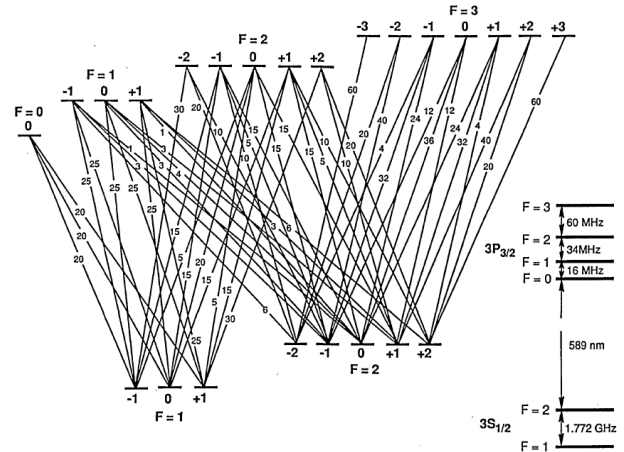Fig.1: Schematic diagram of the sodium D transitions (from Hillman et al.[19]).

Fig. 2: The magnetic substates of the hyperfine levels of the sodium D_2 line. Relative oscillator strengths are indicated (from Ungar[20]).

If only a single frequency laser, tuned to the peak of the D_2 absorption line, is used to excite the sodium atoms, it may be possible to optically pump the atoms from the $F = 2$ to the $F = 1$ ground state. While atoms traveling approximately normal to the laser beam can only cycle between the $F = 2$ ground state and the $F = 3$ upper state until they change direction by collision, atoms moving in other directions can be excited to the $F = 2$ or $F = 1$ upper state. Once excited to these levels, they can fall back either to the $F = 2$ or $F = 1$ ground state, and after only a few cycles will end up trapped in the ground state. About 1% of all atoms get pumped to the $F = 1$ ground state every collision lifetime (100 microseconds). If this were the only process, the layer would become optically transparent in time scale of 0.01 seconds. The significance of this effect depends on how quickly the ground level is rethermalized by collision or the atoms replaced by the mesospheric wind.

Each of the F levels splits up into $2F+1$ magnetic quantum levels in the presence of a magnetic field or linearly or circularly polarized light (Fig. 2). For linearly polarized light only transitions with $\Delta m = 0$ are permitted, whereas for circularly polarized light, Δm must be either $+1$ or -1, depending on the handedness of the light. Atoms in a given m level in the upper state can fall back according to the rule $\Delta m = -1, 0, +1$. If we look at the $F = 2$ ground state $\rightarrow F = 3$ upper state transition we see that the bottom ground state consists of 5 m levels and the upper consists of 7 m levels. If an atom is cycled many times, the selection rules tend to move the atoms towards the $m = 0,\ m = 0$ state for linearly polarized light. If however we use circularly polarized light, the selection rule for absorption is $\Delta m = +1$ (or -1 for the other polarization). After about $6-10$ cycles (excitation-decay) the atoms are pumped into the $m = 2,\ m = 3$ state. The only radiation that can be emitted by the $F = 3,\ m = 3 \rightarrow F = 2,\ m = 2$ transition is circular polarization.

4. EFFECT OF THE GEOMAGNETIC FIELD

In the presence of a magnetic field the simple optical-state linkage pattern of Fig. 2 is exactly applicable for left-circular polarization only when the Earth's magnetic field is parallel to the direction of propagation of the laser beam. The linkage pattern of Fig. 2 requires that the axis of the quantization be the propagation direction, but in the presence of a magnetic field, m is a good quantum number only if the axis is along the magnetic field; i.e., the zero magnetic-field states of Fig. 2 are no longer energy eigenstates when the Earth's magnetic field B, and the laser propagation direction k are not parallel. In the case of the $3^2S_{1/2}$ ground state of Na, the 1772 MHz hyperfine splitting is so much larger than the

Zeeman splitting because of the Earth's magnetic field that the Zeeman eigenstates are approximately the (F, m) states as long as the axis of the quantization is along $\boldsymbol{B}$.

To illustrate theoretically the effect of the geomagnetic field on the circularly polarized pumping of the mesospheric sodium atoms, we use the following derivation from Milonni *et al.*[21]. The interaction Hamiltonian for an atom with angular momentum $\boldsymbol{F}$ in a weak magnetic field $\boldsymbol{B}$ is

$$H_{mag} = g_F\,\mu_B\,\boldsymbol{B}{\cdot}\boldsymbol{F} \tag{2}$$

where μ_B is the Bohr magneton (9.274×10^{-24} J/T), g_F is the Landé factor, and $\boldsymbol{F} = \boldsymbol{I} + \boldsymbol{J}$ is the sum of the nuclear and electronic angular momentum, respectively. For sodium we take Arimondo *et al.*[17]:

$$I = 3/2,$$

$$g_F = g_J[\frac{F(F+1)+J(J+1)-I(I+1)}{2F(F+1)}]\ g_{J=3/2}(3^2P_{3/2})=1.334,$$

$$g_{J=1/2}(3^2S_{1/2})=2. \tag{3}$$

The weak static field $\boldsymbol{B}$ cannot cause transitions between states of different energy, and, in particular, it cannot cause transition between states with different values of F. It will cause transitions only between states with different m and the same F. We label density-matrix elements with the same F by a subscript (F). The density–matrix equations following from the Hamiltonian (2) are then

$$[\dot{\sigma}_{m_1m_2}^{(F)}]_{mag} = -i\sum_{m_3} V_{m_2m_3}^{(F)}\sigma_{m_1m_3}^{(F)} + i\sum_{m_3} V_{m_3m_1}^{(F)}\sigma_{m_3m_2}^{(F)}, \tag{4}$$

where

$$V_{m_2m_3}^{(F)} = \frac{1}{\hbar}\langle m_2|g^{(F)}\mu_B\boldsymbol{B}\boldsymbol{F}|m_3\rangle. \tag{5}$$

The magnetic quantum number m_i is defined with respect to the quantization axis chosen to describe the interaction of the atom with the laser field. In the case of a circularly polarized laser field, this axis is chosen to be along the direction of propagation of the field. Note, however, that the laser field is ignored. Note also that the laser field causes transitions only between states of different energy, so that it does not directly affect the density-matrix equations (4) that refer to states that are degenerate in the absence of any fields.

$V_{m_2m_3}^{(F)}$ is evaluated using a complete orthogonal set of states $|m\rangle$ such that $\mathrm{BF}|m\rangle = Bm|m\rangle$, i.e., the eigenstates of F^2, F_z with the z axis along $\boldsymbol{B}$:

$$V_{m_2m_3}^{(F)} = \frac{1}{\hbar}g^{(F)}\mu_B\boldsymbol{B}\sum_m m\langle m_2|m;R\rangle\langle m;R|m_3\rangle. \tag{6}$$

The label R indicates that the magnetic quantum number is defined with respect to a quantization axis rotated by an angle θ from the quantization axis to which m_2, m_3 refer, θ for our purposes being the angle between the direction of propagation of the laser field $\boldsymbol{k}$ and the direction of $\boldsymbol{B}$. The scalar products appearing in Eq. (6) are the matrix elements of the rotation matrix, Gottfried [22]:

$$\langle m_2|m;R\rangle = d_{m_2m}^{(F)}(\theta).$$

Thus

$$V_{m_2m_3}^{(F)} = \frac{1}{\hbar}g^{(F)}\mu_B\boldsymbol{B}\sum_m md_{m_2m}^{(F)}(\theta)d_{mm_3}^{(F)}(-\theta). \tag{8}$$

For a given magnetic field strength B, the transitions among different m states belonging to each F are described by Eq. (4). The diagonal element $\sigma_{mm}^{(F)}(t)$, for instance, is the probability for the state (F, m) at time t. Numerical solutions of the density-matrix equations (4) are cumbersome. The simplest nontrivial case, $F = 1$, has been solved numerically by Morris [23].

(Fig. 3) shows the population remaining in the $3^2S_{1/2}$ ($F=1$, $m=1$), ground state at normalized time t/τ, where $\tau = 4\pi\hbar/(\mu_B B)$ for various angles between the laser propagation direction and the Earth's magnetic field. From top to bottom the angles are 15°, 30°, 45°, 60°, 75°, and 90°. The atom is prepared in the $3^2S_{1/2}$ ($F = 1$, $m = 1$) ground state at time $t = 0$ and evolves in the presence of the Earth's magnetic field but in the absence of a laser field. Collisions have been neglected so the population is a periodic function of time.
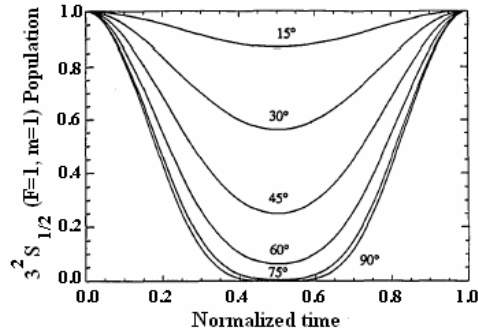

Fig. 3: Representation of the $3^2S_{1/2}$ ($F = 1$, $m = 1$) state population as a function of normalized time, for various angles between the laser propagation direction and the Earth's magnetic field. From Morris [23]

Occupation probabilities of the $3^2S_{1/2}$ ($F = 2$, $m = 2$) state and of the $3^2P_{3/2}$ ($F = 3$, $m = 3$) state (solutions of Eq. (4)) have been calculated by Milonni $et\ al$[20]. These solutions indicate that the geomagnetic field acts to redistribute magnetic sublevel populations in ~1 μs (the magnetic field intensity over Albuquerque is ~$B = 0.51$ G implying $\tau = 2.8$ μs). In these calculations, spontaneous emission and the laser field are ignored.

In 2006 Denman $et\ al$.[24] published experimental results on the dependence of LGS return flux as a function of laser beam direction. The maximum return is observed at the location in the sky where the Earth's magnetic field lines are pointing directly at the SOR, hence when the laser beam propagation in the mesosphere is parallel with $\boldsymbol{B}$. The magnetic field has no effect when the LGS is produced with a linearly polarized beam.
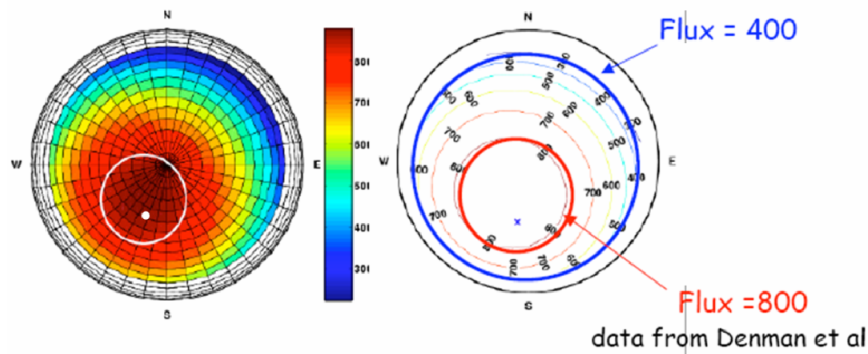

Fig. 4: Radiance return from a 30 W, circularly polarized sodium LGS, Denman $et\ al$.[25].

A complete numerical solution of Eq. (4) for all the values of the angle between the Earth's magnetic field lines and the laser propagation direction should be carried out to study the effect of the Earth's magnetic field on the circularly polarized optical pumping of the mesospheric sodium atoms. As this solution is not available for the moment, we have to suggest another approach.

5. RESULTS

Drummond *et al.*[26] reported that the impact of the Earth's magnetic field on the brightness of the LGS is given by the sine of the angle θ between the laser beam propagation and the direction of the magnetic field lines. Pumping with linear polarization is not affected by the magnetic field, and in fact, pumping with circular polarization with a laser beam propagation perpendicular with the magnetic field lines produces a LGS only as bright as pumping with linear polarization (at least under the conditions at the SOR). The empirical expression for the magnetic field brightness dependence factor for circular polarization is (Denman *et al.*[4]),

$$f = 2.25 - 1.25 \sin(\theta). \tag{9}$$

5.1. Effect of the geomagnetic field

Using Eq. (9) and the characteristics of the Earth's magnetic field over Paranal (Latitude −24.6°, Longitude −70.4°), the declination and the inclination are respectively: 0° and − 21°, we obtain the following (Fig. 5) showing a polar plot of the magnetic field factor *f* in the sky of the VLT site.
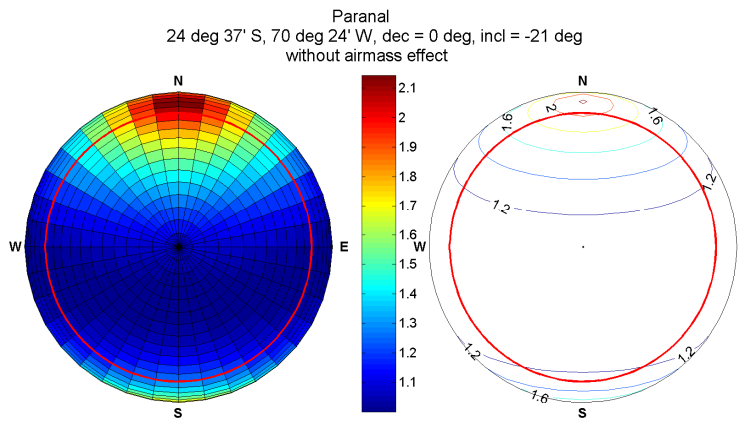

Fig. 5: polar plots of the magnetic field factor *f* in the sky of the VLT site (Paranal).

To compare our results with the experimental measurements of Denman *et al.*[25], we calculate the effect of the geomagnetic field on the enhancement of the sodium laser guide star return due to the optical pumping for the Starfire Optical Rang (SOR) telescope. (Fig. 6) shows the results of our calculations.
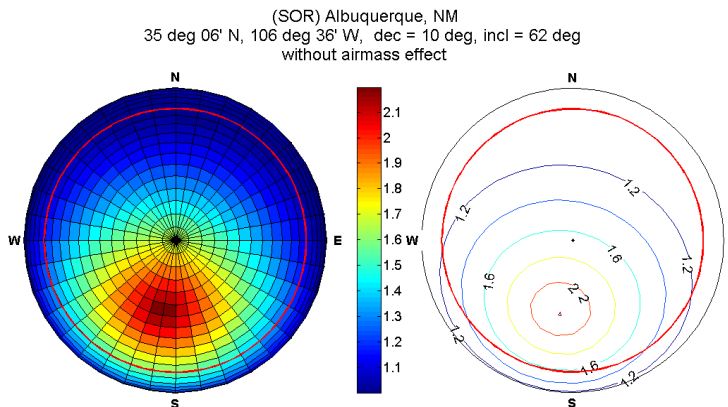

Fig. 6: polar plots of the magnetic field factor *f*, for the SOR telescope (Albuquerque, New Mexico, USA).

Starting from the comparison of our calculations (Fig. 6) with the experimental measurements (Fig. 4), we decide to introduce the effect of the atmospheric transmission on the propagation of the laser beam and on the light received from the sodium laser guide star.

5.2.   Effect of the atmospheric transmission

We assume an atmospheric one–way transmission at 589 nm of

$$T = (T_{at})^{\sec\alpha}, \tag{11}$$

where $T_{at} = 0.84$ is a mean transmission at zenith, α is the zenith angle and $\sec(\alpha)$ is the secans.

5.3.   The effect of the atmospheric transmission and the geomagnetic field

The combined effect of the geomagnetic field and the airmass on the enhancement of the sodium laser guide star return due to the optical pumping is:

$$fT^2 = (2.25 - 1.25\sin\theta)(T_{at})^{2\sec\alpha} \tag{12}$$

Using Eq. (12) we calculate the combined effect of the airmass (atmospheric transmission) and the geomagnetic field on the sodium laser guide star produced by SOR using a single frequency circularly polarized laser. The results of our calculations are presented in (Fig. 7).
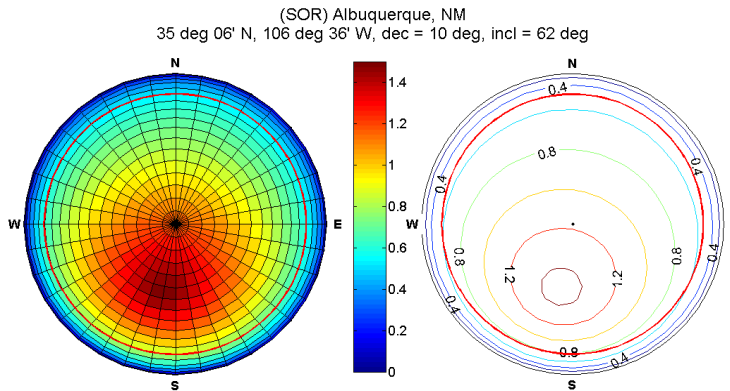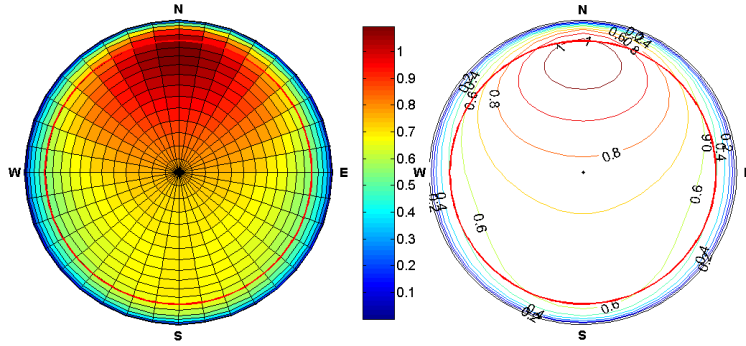

Fig. 7: polar plots of the combined effect of the airmass and the geomagnetic field on a circularly polarized sodium LGS for the SOR telescope (Albuquerque, New Mexico, USA).
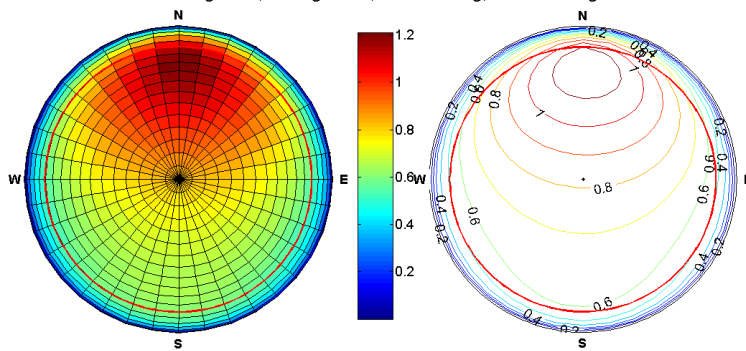
The experimental results of Denman *et al.*[25] (Fig. 4) show that the resultant peak returns are obtained at approximately 198 deg. azimuth and 71 deg. elevation agreeing with our calculations; the expected location of 190° azimuth and 62° elevation (Fig. 7).

Starting from this reasonable agreement between our calculations and the experimental results, we decide to calculate the combined effect of the airmass and the geomagnetic field on the enhancement of the circularly polarized sodium laser guide star return for several telescopes. The results of our calculations are presented in (Fig. 8).
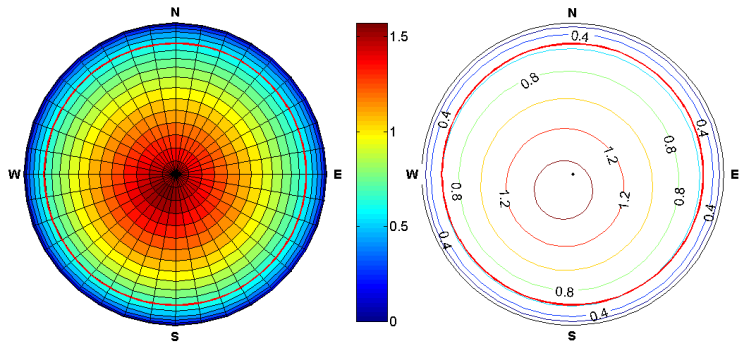
Paranal
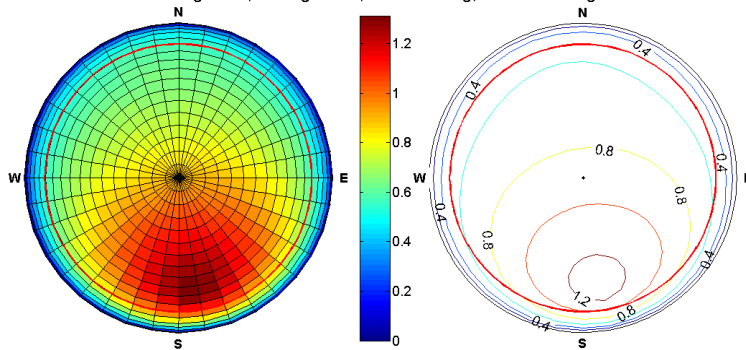24 deg 37' S, 70 deg 24' W, dec = 0 deg, incl = -21 deg

Cerro Pachon
30 deg 14' S, 70 deg 44' W,   dec = 2 deg, incl = -30 deg

Dome C
75 deg 68' S, 123 deg 22' E, dec = -150 deg, incl = -82 deg

La Palma
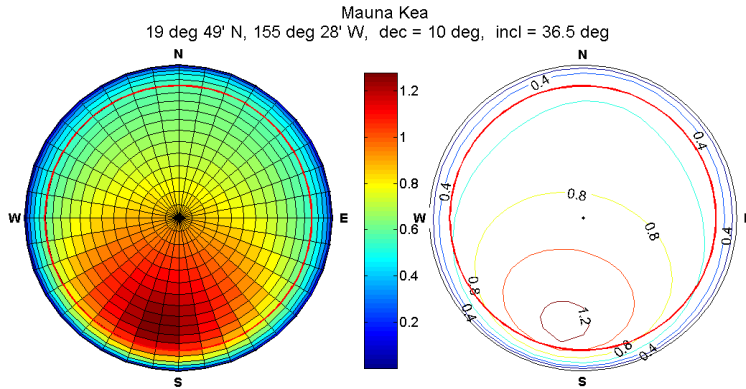28 deg 41' N, 17 deg 56' W, dec = -8 deg, incl = 38.5 deg

Fig. 8: polar plots of the combined effect of the airmass and the geomagnetic field on circularly polarized sodium LGS for several telescopes (from top to bottom: Paranal, Cerro Pachon, Dome C (Antarctica), La Palma, Mauna Kea).

6. CONCLUSION

Optical pumping of the mesospheric sodium atoms with circularly polarized single-frequency CW laser increases the return flux from the LGS. The geomagnetic field acts on the redistribution of magnetic substates, which would reduce the degree of optical pumping and, in the worst case, eliminate the advantage of using circularly polarized laser radiation.

The optical pumping of the mesospheric sodium atoms with circularly polarized laser light is most efficient when the beam is parallel to the geomagnetic field lines. Because northern Chile (VLT, Gemini South etc), Mauna Kea (Keck, Gemini North) and La Palma (GTC) are all located relatively close to the magnetic equator, this direction lies close to the horizon. For single-frequency lasers, the variation of return flux when moving the beam from the direction parallel to the field lines to orthogonal is about a factor of 2.25 Denman *et al.*[4]. For other laser formats, we expect smaller factors.

Most of the published results of LGS return flux refer to directions on the sky close to the optimum. However, we emphasize that the LGS laser power must be budgeted for the direction of minimum return, since we need to be able to observe with LGS-AO in any direction above 30 degrees altitude. *Therefore, we disregard the return benefits of optical pumping in the calculation of the required laser power*.

An interesting point is that the magnetic field in northern Chile is quite weak ($B = 0.23$ G), and hence optical pumping may be disrupted less than at the SOR in Albuquerque, New Mexico ($B = 0.51$ G) or in Hawaii ($B = 0.35$ G) for example. Numerical studies are underway to quantify the return flux further Kibblewhite[27]. Experimental results to assess the effect of the field strength will ultimately be needed.

In thermal equilibrium, the sodium atoms in the $F = 2$ ground state comprise only 5/8 of the total number of atoms. We can introduce a second frequency 1.772 GHz above the primary frequency and thereby excite atoms from the $F = 1$ ground state into upper levels $F = 0$, $F = 1$ and $F = 2$. Atoms in the $F = 1$ and $F = 2$ upper state have a reasonable probability of falling into the lower $F = 2$ level and then being pumped to the $m = +3$ state. We can therefore in principle pump all of the atoms into this state enabling us to use potentially 100% of the atoms rather than the 62.5% that populate the $F = 2$ ground state in thermal equilibrium (backpumping was originally proposed by MIT/LL in the 1980s).

REFERENCES

[1]   Milonni, P. W., Fugate, R. Q., Telle, J. M., "Analysis of measured Photon returns from sodium beacons" J. Opt. Soc. Am. A. **15**, 217–233 (1998).

[2]   Ge, J., *et al*. Proc. SPIE, 3353, 242−254, (1998).

[3]   Rabien, S., Ott, T., Hackenberg, W., *et al*, "The ALFA Laser and Analysis Tools, " ExA 10, **78**, (2000).

[4]   Denman, C., private communication, May (2008).

[5]   Quivers, W. W., "Production of Highly polarized vapors using laser optical pumping with velocity changing collisions", Phys. Rev. A **34**, 3822, (1986).

[6]   http://www.geomag.bgs.ac.uk

[7]   Plane, J. M. C., International Rev. in Physical Chemistry, Vol. **10**, No. 1, 55 (1991).

[8]   Davis, D. S., Hickson, P., Herriot, G., and She, C.-Y., "Temporal variability of the telluric sodium layer", Opt. Lett., **31**, p. 3369–3371(2006).

[9]   Kibblewhite, E. J., "Laser Guide Star Adaptive Optics for Astronomy," Edited by N. Ageorges, and C. Dainty. Kluwer Academic Publishers (Dordrecht), p.51, (2000).

[10]   Gardner, C. S., Voelz, D. G., Sechrist, C. F. Jr., & A. C. Segal, J. Geophys. Res.**91**, 13659, 1986.

[11]   Fricke, K. H. and Von Zahn, U., "Mesopause Temperature Derived from Probing the Hyperfine Structure of the D2 Resonance Line of Sodium by Lidar," J. Atmos. Terr. Phys. **47**,499 (1985).

[12]   Jeys, T. H., the Lincoln Lab. Journal, 4, 123, (1991).

[13]   Clemesha, B. R., Takahashi, H., Upper atmosphere research at INPE, Adv. Space Res. **16**, 141, (1995).

[14]   Qian, J., Gardner, C. S., "Simultaneous lidar measurements of mesospheric Ca, Na, and temperature profiles at Urbana, Illinois". J. Geophys. Res. **100**, 7453, (1995).

[15]   Clemesha, B. R., Batista, P. P., Simonich, D. M., "Formation of sporadic sodium layers," J. Geophys. Res. **101**, 19701, (1996).

[16]   Butler, D. J., Davies, R. I., Fews, H., *et al*., "Sodium layer monitoring at Calar Alto by LIDAR," In: Wizinowich P. L. (ed.), Adaptive Optical Systems Technology, Proc. SPIE 4007, 358, (2000).

[17]   O'Sullivan, C., Redfern, R. M., Ageorges, N., *et al*., "Short timescale variability of the mesospheric sodium layer," ExA 10, 147, (2000).

[18]   Arimondo, E., Inguscio, M., & P. Violino, Rev. Mod. Phys. 49, 31 (1977).

[19]   Hillman, P. D., Drummond, J. D., Denman, C. A., Fugate, R. Q., "Simple Model, including Recoil, for the Brightness of Sodium Guide Stars created from CW Single Frequency Fasors and Comparison to Measurements," SPIE, Marseille, Paper No. 7015−22 (2008).

[20]   Ungar, P. J., Weiss, D. S., Riis, E., and Chu, S., "Optical molasses and multilevel atoms : theory," J. Opt. Soc. Am. B. Vol. **6**, No. 11, November (1989).

[21]   Milonni, P. W., Fearn, H., Telle, J. M., Fugate, R. Q., "Theory of continuous-wave excitation of the sodium beacon," J. Opt. Am. A. Vol. **16**, No. 10, October (1999).

[22]   Gottfried, K., *Quantum Mechanics*, (Benjamin, Reading, Mass., 1977), p. 269.

[23]   Morris, J. R., "Efficient excitation of a mesospheric sodium laser guide star by intermediate-duration pulses," J. Opt. Soc. Am. A. Vol. **11**, No. 2, 832−845, February (1994).

[24]   Denman, C. A., Drummond, J. D., Eickhoff, M. L., Fugate, R. Q., Hillman, P. D., Novotny, S. J., Telle, J. M., "Characteristics of sodium guidestars created by the 50-watt FASOR and first closed-loop AO results at the Starfire Optical Range," Proc. SPIE. 6272, 62721L−12, (2006).

[25]   Denman, C. A., Moore, G., Drummond, J. D., Eickhoff, M. L., Hillman, P. D., Telle, J. M., Novotny, S. J., Fugate, R. Q., " Two-Frequency Sodium Guide star Excitation at the Starfire Optical Range," CFAO, workshop (2006).

[26]   Drummond, J. D., Novotny, S. J., Denman, C. A., Hillman, P. D., Telle, J. M., Eickhoff, M. L., Fugate, R. Q., "The Sodium LGS Brightness Model over the SOR," AMOS Technical Conference, (2007).

[27]   Kibblewhite, J. E., "Calculation of returns from sodium beacons for different types of laser," SPIE, Marseille, Paper No. 7015−21, (2008).